

FIELD DEPLOYMENT OF A NANOGAP GAS SENSOR FOR CROP DAMAGE DETECTION

Shakir-ul Haque Khan¹, Mohit Karkhanis¹, Bryan Hatasaka¹, Sayali Tope¹, Seungbeom Noh¹, Rana Dalapati², Ashrafuzzaman Bulbul¹, Ravi V. Mural³, Aishwaryadev Banerjee¹, KyeongHeon Kim⁴, James C. Schnable³, Mingyue Ji¹, Carlos H. Mastrangelo¹, Ling Zang², and Hanseup Kim¹

¹Electrical and Computer Engineering, University of Utah, Salt Lake City, UT 84112

²Materials Science and Engineering, University of Utah, Salt Lake City, UT 84112

³Department of Agronomy and Horticulture, University of Nebraska, Lincoln, NE 68588

⁴Department of Convergence Electronic Engineering, Gyeongsang National University, South Korea, 52828

ABSTRACT

This paper reports the first in-field detection of actual hexanal from the damaged sorghums using the field-deployed nano-gap gas sensor. The previously developed nano-gap gas sensor was fully integrated with electronics and wireless communication units into a portable prototype (10×10×7 cm³). The field deployed gas sensor prototype successfully detected the 'scream' from the mechanically damaged sorghums by detecting a particular gas molecule, hexanal, released after the time point of 3.5 hours since the start of leaf cutting. The sensor prototype was pre-programmed to detect >100 ppm concentrations of hexanal in ambient air. After 1.5 hours since the cutting was stopped, the sensor prototype successfully recovered. The sorghum field testing conditions included a temperature (25~120 °C) and humidity (≤70%RH). The detection demonstration clearly indicated that (1) a prototype successfully captured actual hexanal released from the damaged sorghums real-time and that (2) it was feasible to monitor a mechanically-stressed status of sorghums by gas monitoring.

KEYWORDS

Gas sensor, crop damage, field demonstration, sorghum

INTRODUCTION

Crop yield from precision agriculture can be significantly improved by monitoring early-stage crop damages. Crop damage monitoring can alleviate some of the 35 % crop yield that is affected annually by pests [1]. Such detection had a market size of \$3.86 billion in 2020 and is expected to keep on increasing to reach \$6.97 billion in 2026 [2].

However, the timing and location of the crop damages are difficult to identify due to non-real-time and non-spatial sensing methods such as manual scouting and unmanned sensors [3]. Manual scouting involves being physical presence at the damaged spot in a farm and has been traditionally used to detect the occurrences of insects, microbes and weeds [4]. Unmanned sensing methods such as satellite imaging, spectroscopy and IR sensors have been developed to address the needs for more autonomous sensing [5]. These methods are however often affected by the post processing requirement for image/spectroscopy, environmental condition susceptibility for IR, which make them difficult to utilize in real-time sensing, and limited

accuracy.

Detection of signature VOC gases indicating crop damages has been increasing interest, while such conventional methods have been limited time- and space-wisely [6]. VOC sensing through gas sensors could enable continuous, in-situ monitoring of crops and provide early warning for pest attacks [7]. This is because gas sensors unlike other pest monitoring or scouting methods do not require a user to be present in the field as in imaging methods or require sampling as in chromatographic methods.

The previously reported nanogap-based sensor has demonstrated the detection capability of hexanal only in the laboratory environment so far [8]. Accordingly, it was not a self-standing unit since it did not include supporting electronics for wake-up and wireless communication functions. Additionally, it was under a question about operation stability under the actual field conditions such as humidity and varying temperatures. To investigate into such stability issues, the prototype was deployed in the actual sorghum field in the Nebraska, Lincoln.

This paper reports our initial in-field demonstration of the developed nanogap-based sensor under actual field conditions. Specifically, it reports the operation principle, prototype integration and field experimental conditions and measurement results.

OPERATION PRINCIPLE

The operation of a nanogap sensor prototype starts with the capture of target molecules, hexanal, via the previously developed nano-gap sensor. The capture of molecules leads to the wake-up of the signal processing electronics that includes a fA amplifier, a comparator, and a microcontroller that produces a detection signal. The detection signal is then transmitted to the gateway node using the LoRa module, and finally, to the central station using the LTE network.

FABRICATION AND INTEGRATION

The nanogap-sensor was first fabricated and then functionalized with the hexanal-binding linkers (Fig.1). The nanogap-sensor was, then, integrated into the portable prototype with electronics (Fig. 2).

Nanogap Gas Sensor

The gas sensor fabrication was performed following

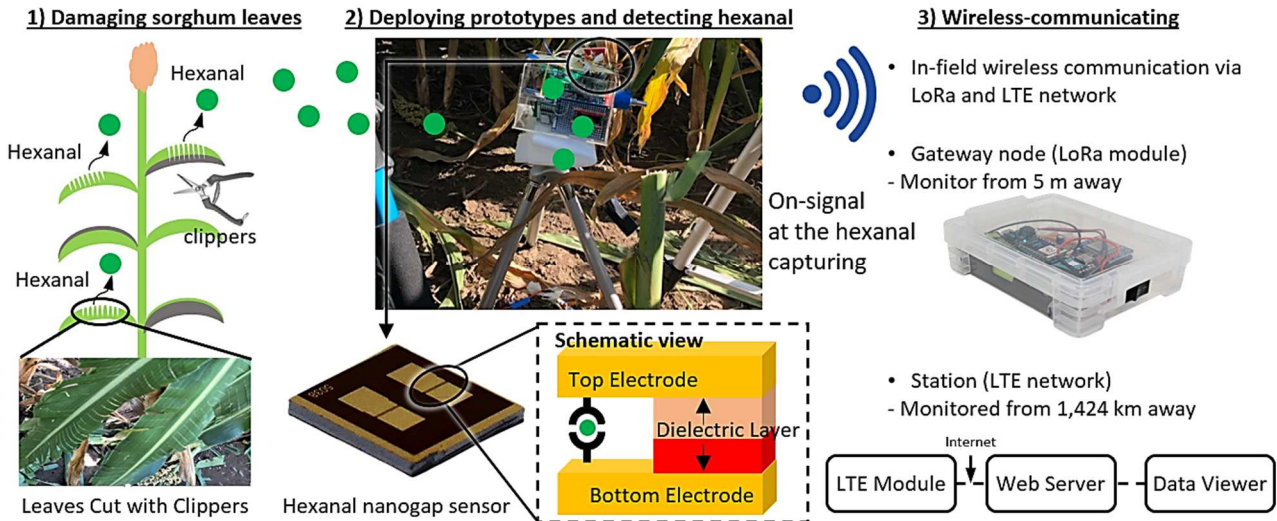


Figure 1: Sensor deployment in a sorghum farm and testing of sensor response to VOCs released from damaged plants

the previously reported protocol [11,12]. The fabricated sensor was coated with a hexanal-sensitive chemistry and then mounted on a bond pad that provided a wire-bonding location during the assembly of the whole prototype.

Prototype Integration

The prototype consisted of the nanogap-sensor, a fA amplifier, a comparator, a microcontroller, an LED, a wireless communication unit and a battery. The integrated amplifier (LMP7721, Texas Instruments) converted the pico-ampere current from the nano-gap gas sensor into milli-voltage signal. The comparator (OPA348, Texas Instruments) generated 0 V or 4.5 V according to the transmitted voltages from the amplifier. The generated signal was used to determine whether the detection event occurred or not. The microcontroller (Teensy 3.6, PJRC), then, converted the input voltage signals into status of not detected or detected and sent them to the LED and LoRa module. The LED displayed the on-signal at the hexanal capturing only. The LoRa module (RFM95x, Adafruit) transmitted the status signal to the gateway with a frequency of 915 MHz. Finally, the prototype was power-supplied by a LiPo battery (2500 mAh, 3.7V).

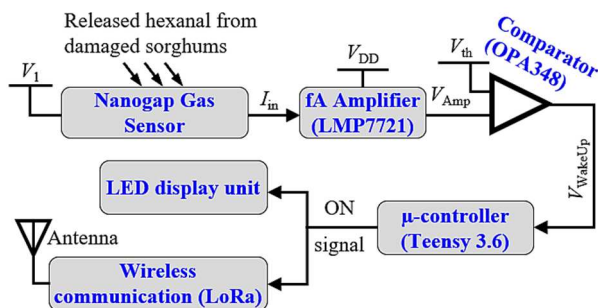


Figure 2: Diagram of the integrated prototype with nano-gap gas sensor

EXPERIMENTS

Operational Range of Temperature and Humidity

Before field deployment, the nanogap-based sensor's operational range of temperature and humidity was pre-defined via in-lab testing. This in-lab testing was performed to compare the sensor operation to potential field conditions. Monitoring of the operation range of the nanogap sensor was performed by varying the humidity and temperature to which the sensor was exposed. Temperature levels were set from 25 °C to 120 °C, and humidity levels were set from 30% to 90% RH. At each temperature and humidity level, the sensor signal output was measured while being exposed to commercial hexanal in 100 ppm that was our hypothesized field concentration. The sensor's output signal was measured by Keithely semiconductor spectrometer, and the changes in sensor response were monitored before and after the exposure to hexanal.

In-Field Hexanal Detection

In-field hexanal detection with the nanogap sensor integrated into the prototype was performed in the sorghum field containing 4 months old sorghums. Four different prototypes were deployed: one prototype was the working sensor and three prototypes were controls that were not expected to respond to the hexanal exposure. After the prototypes were deployed in the field, the sorghum leaves were cut at the constant rate of 91 cuts per 1 minute for 210 minutes. The hexanal detection at the nanogap sensor was continuously monitored at the prototype as well as at a remote place that was wirelessly tethered to the implemented prototypes.

RESULTS

Operational Range of Temperature

The in-lab testing results indicated the sensor's operational range for temperature was from 25 °C to 120 °C, as shown in Fig. 3. Within these temperature ranges,

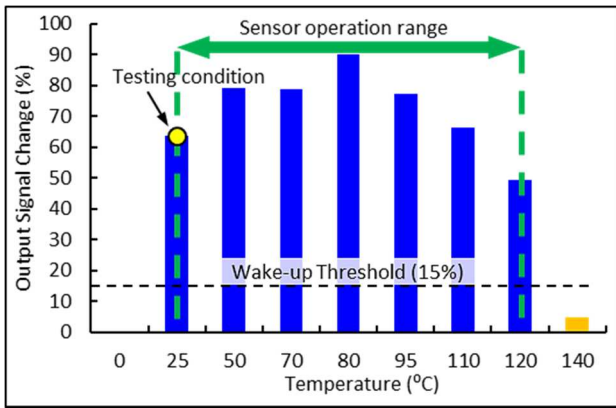


Figure 3: Sensor signal change with increasing temperature

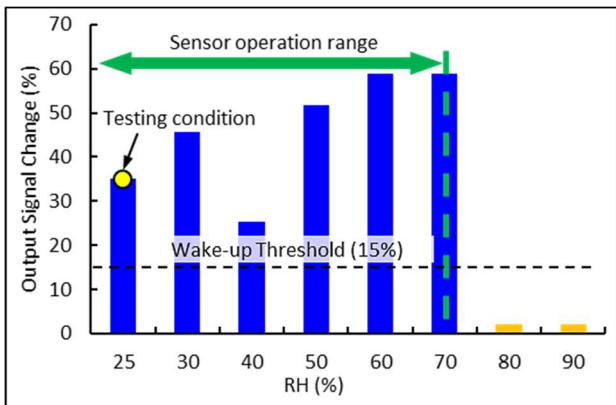


Figure 4: Sensor signal change with increasing humidity

the sensor produced an output signal, which was the ratio of resistance, exceeding 1.15 or 15% that was utilized as a threshold for an electronics wake-up.

As the temperature around the sensor increased from room temperature, the output signal, an on/off ratio of resistance, rose gradually until 80 °C. During this temperature testing, the change in sensor output increase from 63.68% at 25 °C to 90.13% at 80 °C by a ratio of 1.38 times. Beyond the temperature values of 80 °C, the sensor output change started to drop, reaching 77.29% at 95 °C, 66.41% at 110 °C and finally 49.24% at 120 °C. Even at 120 °C with a output change of 49.24% the sensor was still considered to be usable as it was more than 3 times the noise value of 15%. These results confirmed our hypothesis that (1) increased temperature led to higher energy and more frequent penetration of a target molecule into a nano-gap until the ambient becomes 80 °C, and that (2) beyond 80 °C, the thiol bonding of a chemical linker to the gold surface in a nano-gap sensor started be damaged, thus resulting in decreasing output signals.

Operational Range of Humidity

The sensor's operational humidity range was also identified during the in-lab testing before field deployment, as shown in Fig. 4. Figure 4 showed that the sensor was able to operate at a wide humidity range from 25% to 70%. As the humidity level increased, the output remained relatively stable between 30% to 70% humidity except at a relative humidity range of 40%: 45.65% at 30% RH, 51.72% at 50% RH, 58.85% at 60% and 59% at 70% RH.

The data point at RH 40% will be investigated further. Beyond humidity values of 70% the sensor response to hexanal was lower than the noise value of 15% and was, thus, considered to be unstable at those levels. It is hypothesized that the hydrogen bond of water molecules near the linker could inhibit the sensor's capturing of the hexanal as explained in [15].

In-Field Detection of Actual Hexanal

The field deployed nanogap sensor captured the actual hexanal from the damaged sorghums after 3.5 hours exposure time in the field, and then recovered back after 1.5 hours recovery time, as shown in Fig.5. Subsequently, the prototype successfully transmitted the detection signal to the LED display unit and the LoRa wireless communication unit. The in-field testing was performed at field conditions of 25 °C and 25 % RH.

Figure 5 showed the overall timeline of the hexanal detection from sensor installation and cutting the sorghums leaves to the recovery of the prototype once removed from the field. The sorghum field where the deployment took place contained 4 months old sorghum plants. The deployed prototype transmitted a gas detection signal after 3.5 hours of continuous cutting of sorghum leaves, when 80 plant leaves were cut. The LED unit of the prototype displayed a gas detection message of on-signal simultaneously. The deployed prototype was removed from around the sorghum plants at the 5.0 hour mark, at which point the sensor recovery was observed. During the whole deployment process the three control prototypes did not respond.

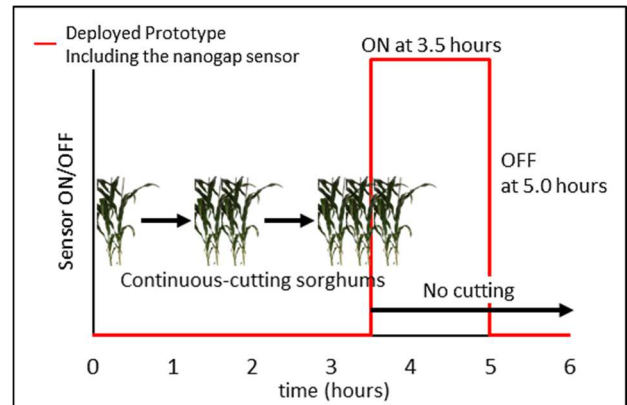


Figure 5: Timeline for actual hexanal detection in field

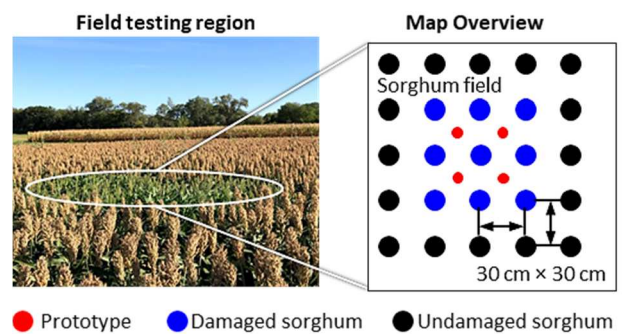


Figure 6: Timeline for actual hexanal detection in field

CONCLUSION

This paper reported the demonstration of an in-field hexanal detection enabled by the previously-developed nano-gap based sensor prototype. In-lab testing of the sensor pre-identified the operation range of the sensor as from 25 °C to 120 °C in temperature and below 70% RH in humidity. The integrated prototype demonstrated the detection of the sorghum damages after 3.5 hours. The nanogap sensor was also able to recover back to initial status after 1.5 hours of recovery time. The wireless communication from the prototype to a remote central station was validated by the received messages through a gateway node via an LoRa module and LTE network.

ACKNOWLEDGEMENTS

This research work was generously supported by the cooperative agreement of DE-AR0001064 of the ARPAE OPEN 2018 program (Program Manager: Dr. David Babson). The initial development of a nano-gap sensor was generously supported by cooperative agreement of HR0011-15-2-0049 of the DARPA NZERO program (Program Manager: Drs. Roy Olsson and Benjamin Griffin). Microfabrication was performed at the state-of-the-art Utah Nanofabrication Facility in the University of Utah.

REFERENCES

- [1] "Studies in Agricultural Economics No.113" Research Institute of Agricultural Economics Committee on Agricultural Economics, Hungarian Academy of Sciences, 2011.
- [2] "Pest Control Market Size In 2021 : Top Countries Data with 8.8% CAGR, Global Industry Brief Analysis by Top Key companies and Growth Insights to 2027 | Latest 117 Pages Report", Report from KTVN News, Oct 12 2021.
- [3] Prince P, Hill A, Piña Covarrubias E, Doncaster P, Snaddon JL, Rogers A. Deploying Acoustic Detection Algorithms on Low-Cost, Open-Source Acoustic Sensors for Environmental Monitoring. *Sensors*. 2019; 19(3):553.
- [4] Adedeji, Akinbode et. al "Non-Destructive Technologies for Detecting Insect Infestation in Fruits and Vegetables under Postharvest Conditions: A Critical Review" (2020).
- [5] López O, Rach MM, Migallon H, Malumbres MP, Bonastre A, Serrano JJ. Monitoring Pest Insect Traps by Means of Low-Power Image Sensor Technologies. *Sensors*. 2012; 12(11):15801-15819.
- [6] L.M. Seitz and D. B. Sauer "Volatile Compounds and Odors in Grain Sorghum Infested with Common Storage Insects", *Cereal Chem*. 73(6):744-750.
- [7] Scala A, Allmann S, Mirabella R, Haring MA, Schuurink RC. Green leaf volatiles: a plant's multifunctional weapon against herbivores and pathogens. *Int J Mol Sci*. 2013;14(9):17781-17811. Published 2013 Aug 30.
- [8] S. -u. H. Khan et al., "Development of a Gas Sensor for Green Leaf Volatile Detection," 2021 21st International Conference on Solid-State Sensors, Actuators and Microsystems (Transducers), 2021, pp.

250-253.

- [9] "Summer Temperature Trends in the Contiguous U.S.", Climate Central
- [10] "Oh The Humidity. Which State Is The Most Humid?" Forbes.
- [11] A. Banerjee, S.H. Khan, S. Broadbent, A. Bulbul, K.H. Kim, S. Noh, R. Looper, C.H. Mastrangelo, H. Kim "Molecular Bridge-Mediated Ultralow-Power Gas Sensing" *Nature Microsystems and Nanoengineering*, 2021.
- [12] Banerjee, A.; Khan, S.H.; Broadbent, S.; Likhite, R.; Looper, R.; Kim, H.; Mastrangelo, C.H. Batch-Fabricated α -Si Assisted Nanogap Tunneling Junctions. *Nanomaterials* 2019, 9, 727.
- [13] Dissociation and Degradation of Thiol-Modified DNA on Gold Nanoparticles in Aqueous and Organic Solvents Nishi Bhatt, Po-Jung Jimmy Huang, Neeshma Dave, and Juewen Liu *Langmuir* 2011 27 (10), 6132-6137.
- [14] Kinetics of the Thiol-Disulfide Exchange Antonino Fava, Antonio Iliceto, and Ettore Camera *Journal of the American Chemical Society* 1957 79 (4), 833-838.
- [15] Liu P, Harder E, Berne BJ. Hydrogen-bond dynamics in the air-water interface. *J Phys Chem B*. 2005 Feb 24;109(7):2949-55.

CONTACT

*Hanseup Kim, tel: +1-801-5879497;
hanseup.kim@utah.edu